Appl. Magn. Reson. 30, 345–358 (2006)

Applied Magnetic Resonance

Towards an Identification of Chemically Different Flavin Radicals by Means of Their *g*-Tensor

A. Schnegg[1], A. Okafuji[1], A. Bacher[2], R. Bittl[1], M. Fischer[2,a], M. R. Fuchs[1,b], P. Hegemann[3], M. Joshi[2], C. W. M. Kay[1,c], G. Richter[2,d], E. Schleicher[1], and S. Weber[1]

[1] Fachbereich Physik, Freie Universität Berlin, Berlin, Germany
[2] Lehrstuhl für Organische Chemie und Biochemie, Technische Universität München, Garching, Germany
[3] Institut für Biologie und Experimentelle Biophysik, Humboldt-Universität zu Berlin, Berlin, Germany

Received September 4, 2006

Abstract. The *g*-tensors of two chemically different flavin mononucleotide (FMN) radicals, one of which is covalently bound via N(5) of its 7,8-dimethyl isoalloxazine moiety, and the other one non-covalently bound to mutant LOV domains of the blue-light receptor phototropin, LOV1 C57M and LOV2 C450A, respectively, have been determined by very high microwave frequency and high magnetic field electron paramagnetic resonance (EPR) performed at 360 GHz and 12.8 T. Due to the high spectral resolution of the frozen-solution continuous-wave EPR spectra, the anisotropy of the *g*-tensors could be fully resolved. By least-squares fittings of spectral simulations to experimental data, the principal values of *g* have been established: $g_X = 2.00554(5)$, $g_Y = 2.00391(5)$, and $g_Z = 2.00247(7)$ for the N(5)-alkyl-chain-linked FMN radical in LOV1 C57M-675, and $g_X = 2.00427(5)$, $g_Y = 2.00360(5)$, and $g_Z = 2.00220(7)$ for the noncovalently bound FMN radical in LOV2 C450A-605. By a comparison of these values to the ones from the flavin adenine dinucleotide radicals in two photolyases, the radical in LOV2 C450A-605 could be clearly identified as a neutral FMN radical, $FMNH^{\bullet}$. In contrast, LOV1 C57M-675 exhibits significantly shifted principal components of *g*, the differences being caused by spin–orbit coupling of the nearby sulfur from the reactive methionine residue, and the modified chemical structure due to the covalent attachment at N(5) of the radical to the apoprotein. The results clearly show the potential of using the *g*-tensor as probe of the global electronic and chemical structure of protein-bound flavin radicals.

---

[a] Present address: Institut für Biochemie und Lebensmittelchemie, Universität Hamburg, Hamburg, Germany
[b] Present address: Institut für Kristallographie c/o BESSY, Freie Universität Berlin, Berlin, Germany
[c] Present address: Department of Biology, University College London, London, United Kingdom
[d] Present address: School of Chemistry, Cardiff University, Cardiff, United Kingdom

1 Introduction

Since their discovery and chemical characterization in the early 1930s [1, 2], flavins have been have been found to be among the most ubiquitous cofactors in nature [3]. With their three oxidation states, fully oxidized (Fl^{ox}), one-electron reduced ($FlH^{\bullet}$ or $Fl^{\bullet -}$), or fully (two-electron) reduced (FlH_2), flavins are involved in one-electron transfer processes and two-electron transfer processes. They are known as versatile compounds which can function both as electrophiles or nucleophiles and that can even form covalent adduct intermediates [4]. Flavins are involved in the production of light in bioluminescent bacteria and are intimately connected with blue-light-initiated processes such as plant phototropism [5, 6], the resetting of the circadian clock [7–10], and enzymatic nucleic-acid repair reactions [9, 11, 12]. The enormous versatility of flavin-containing proteins is clearly due to protein–cofactor interactions that modulate the electronic structure of the flavin cofactor to optimize it for its specific task.

By far the most flavoproteins bind their cofactor in a freely dissociable form. However, in recent years, quite a number of flavoenzymes have been described in which a covalent attachment of the flavin to the protein was recognized (for reviews, see refs. 13 and 14). Several types of covalent flavin adenine dinucleotide (FAD) or flavin mononucleotide (FMN) linkage to the protein have been discovered, the most frequent being the ones with an attachment of the flavin's isoalloxazine ring to the protein either via the 8α-methyl group [15–17] or the C(6) atom [18, 19]. Furthermore, some flavoproteins are known to form covalent adduct intermediates at C(4a) [4, 20, 21] or N(5) [22, 23]. Covalent flavoproteins are generally identified by means of acid precipitation followed by proteolytic fragmentation of the polypeptide. Flavin-linked peptides are subsequently identified by fluorescence emission at acid pH before and after oxidation with performic acid. From their optical absorption spectra, the type of flavin binding cannot be easily derived. In the oxidized state, only minor differences in the major absorbance bands around 450 nm occur. In the radical state, on the other hand, large distributions of the absorption maxima are encountered, depending on interactions of the flavin with the local protein environment, covalent or noncovalent binding and/or its protonation state. No simple correlation between the position of the long-wavelength absorptions and the type of flavin radical has been found to date.

With the advent of recent technology to record electron paramagnetic resonance (EPR) spectra at ever-higher microwave frequencies and correspondingly stronger magnetic fields and consequently the ability to resolve g-tensors of organic radicals at high accuracy, the question arises as to whether the g-tensor is a good parameter for an identification of the type of flavin radical. For neutral flavin radicals in the DNA repair enzyme photolyase, we have shown recently that at 95 and 360 GHz the principal components of g can be resolved and its principal axes assigned to the molecular frame of the 7,8-dimethyl isoalloxazine moiety of the flavin [24–27]. We focus in this contribution on two chemically different flavin radicals in a comparable protein environment (which

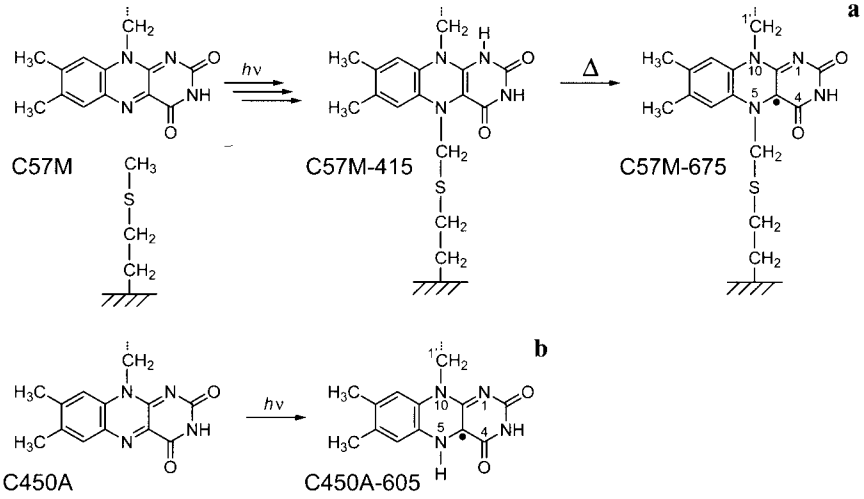

Fig. 1. Formation of neutral FMN radicals in LOV domains of phototropin. **a** Irreversible photoreduction of FMN in *C. reinhardtii* LOV1 C57M. After excitation of the FMN to the triplet state, its reaction with the terminal methyl group of methionine-57 leads to the formation of the photoadduct C57M-415. Slow thermal oxidation of the adduct generates the neutral flavoprotein radical C57M-675 (for further details, see refs. 23 and 28). **b** Photoreduction of FMN in *A. sativa* LOV2 C450A (for further details, see refs. 29 and 30).

is however unrelated to the photolyases), with the aim to find out if the radicals can be distinguished by their *g* parameters. As paradigm systems we have chosen (i) an FMN radical that is covalently linked at N(5) of its isoalloxazine ring to the protein backbone in the LOV1 (light, oxygen, and voltage) domain of algal (*Chlamydomonas reinhardtii*) phototropin and (2) a noncovalently bound FMN radical in the related LOV2 domain of *Avena sativa* phototropin. The former is generated by an irreversible light reaction of a LOV1 mutant, C57M, followed by thermal treatment [23, 28] (Fig. 1a), and the latter by photoreduction of the LOV2 C450A mutant, which has been described previously to occur in the presence or absence of an exogenously added electron donor [29, 30] (Fig. 1b). Both mutant LOV domains have been previously characterized by X- and W-band EPR and electron–nuclear double resonance (ENDOR) spectroscopy and found to be charge neutral on their redox-active isoalloxazine ring [28, 29]. The wild types of both domains undergo covalent adduct formation with a functional cysteine in the immediate surroundings of the FMN as the primary photoreaction in blue-light photoreception of phototropin [20, 31, 32].

2 Materials and Methods

***Chlamydomonas reinhardtii* LOV1 C57M.** The preparation of the recombinant LOV1 C57M domain of *C. reinhardtii* phototropin followed procedures that have

been described previously [28, 33]. The protein sample was then illuminated under anaerobic conditions with light of 420–480 nm from a filtered Xe lamp (ILC PS800SW-1) and afterwards warmed to 40 °C for 4 h to yield LOV1 C57M-675.

***Avena sativa* LOV2 C450A.** The preparation of the recombinant LOV2 C450A domain (amino acid residues 405 to 559) of *A. sativa* phototropin followed procedures that have been reported elsewhere [20, 29]. Photoreduction was performed with blue light of 420–480 nm from a filtered halogen lamp (Streppel WL-25, Wermelskirchen-Tente, Germany) to yield LOV2 C450A-605.

EPR Spectroscopy. EPR spectra were recorded with a laboratory-built superheterodyne quasi-optical spectrometer (360 GHz, 12.8 T) [34], consisting of a 14 T superconducting magnet (Oxford Teslatron) and a 360 GHz heterodyne microwave board (Farran Technologies and Radiometer Physics). Spectra were either recorded using a Fabry-Pérot type resonator (LOV1 C57M) or without microwave resonator in induction mode with a small amount (9 μl) of sample (LOV2 C450A) placed onto a sample holder. To ensure high yield of flavin radicals, the samples were irradiated in situ with blue light from a filtered halogen lamp (Streppel WL-25). The probe head was then introduced into the precooled static helium contact cryostat (Oxford Instruments CF1200) inside the superconducting magnet and rapidly cooled to 160 K.

Spectral simulations. To calibrate the magnetic field, the six-line EPR spectrum from a Mn(II)/MgO standard, which was incorporated in a polystyrene matrix and placed in the proximity of the protein sample, was recorded simultaneously with the protein samples. The EPR spectrum was simulated following the procedure described by Burghaus et al. [35]. In order to obtain the un-

Table 1. EPR parameters used in the simulations of the 360 GHz EPR spectra of the neutral FMN radicals in mutant LOV domains of phototropin (see Figs. 4 and 5). For both radicals, anisotropic hyperfine couplings of $(A_\perp, A_\parallel) = (-0.06$ mT, 1.53 mT) and (0.04 mT, 0.83 mT) for the nitrogens N(5) and N(10), respectively, have been taken into account [36]. For LOV2 C450A-605, the hyperfine tensor of H(5), $(A_x, A_y, A_z) = (-0.49$ mT, -1.32 mT, -0.9 mT) has been used in the simulations. For LOV1 C57M-605, an isotropic hyperfine coupling of -0.62 mT for the two β-protons of the $-CH_2-S-$ side chain at N(5) has been taken into account [28].

Parameter		Value for:	
		FMNH$^\bullet$ in *A. sativa* LOV2 C450A-605	FMN$^\bullet$ in *C. reinhardtii* LOV1 C57M-675
g-Tensor	g_X	2.00427(5)	2.00554(5)
	g_Y	2.00360(5)	2.00391(5)
	g_Z	2.00220(7)	2.00247(7)
$\lvert\delta\rvert$		(8±2)°	n.a.
Inhomogeneous residual line width (mT)	Γ_X	0.78(4)	3.7(7)
	Γ_Y	0.93(4)	1.3(4)
	Γ_Z	1.05(1)	1.1(1)

distorted EPR spectrum of the frozen protein solution, the manganese spectrum was subsequently subtracted after calibration, or the spectrum of a sample without Mn(II)/MgO standard was measured. The 360 GHz EPR spectra were simulated using the program "fx-fitx" described in detail elsewhere [36]. A least-squares fitting algorithm yielded the best agreement between simulated and experimental data for the parameter sets given in Table 1. In the starting parameter sets of the fitting procedure, the hyperfine couplings of the nitrogens N(5) and N(10) were fixed. The hyperfine coupling of the position 5 proton in LOV2 C450A-605 was taken from pulsed ENDOR spectra recorded at X-band microwave frequencies. The flavin radical generated from LOV1 C57M is lacking a proton at N(5). Instead, the hyperfine couplings of two β-protons relative to N(5) as obtained from pulsed ENDOR spectroscopy [28] were used in the simulations. The canonical values of the g-tensor, g_X, g_Y, and g_Z (X, Y, and Z are the principal axes of g), the orientation-dependent residual line widths Γ_X, Γ_Y, and Γ_Z along the principal axes of g, and the angle $|\delta|$ (see ref. 27, fig.1) between the A_y component of the hyperfine tensor A(H(5)) in LOV2 C450A-605 (x, y, and z are the principal axes of A(H(5))) and g_Y were varied over a wide range of physically plausible values. The nonlinear least-squares fit routine is based on a trust-region reflective Newton algorithm (Matlab, The Mathworks).

3 Results and Discussion

3.1 UV/vis Spectroscopy

Flavin cofactors show characteristic optical absorption properties in all three biologically relevant redox states. Proteins with flavin chromophores are frequently isolated in a yellow-colored form, which is characteristic for their flavin cofactor being in the fully oxidized state Fl^{ox}. Absorption maxima in a narrow distribution around 450 and 370 nm represent the $S_0 \rightarrow S_1$ and $S_0 \rightarrow S_2$ transitions of the flavin, respectively. Well-resolved vibration side bands are indicative of tight and well-defined noncovalent binding of the chromophore to the protein structure. Flavin radicals by comparison show absorption maxima in a wider range between about 500 and 700 nm that render paramagnetic flavoproteins bluish to red depending on the protonation state of their flavin cofactor. If the protein-bound flavin is not easily accessible to molecular oxygen, such radicals may be stable on a time scale of hours or even longer. In Fig. 2, we have collected the optical absorption spectra of four blue-light-active flavoproteins with their redox-active chromophore in the radical form. The spectra of two different DNA photorepair enzymes, cyclobutane-pyrimidine dimer (CPD) repairing CPD photolyase of *Escherichia coli* and the (6–4) photoproduct repairing (6–4) photolyase of *Xenopus laevis*, are shown in Fig. 2a. The FAD cofactors of both photolyases have been unambiguously identified as neutral radicals by identification of their position 5 proton hyperfine coupling in pulsed ENDOR experiments at X-band and W-band frequencies [26, 37]. The CPD photolyase and the (6–4) photolyase

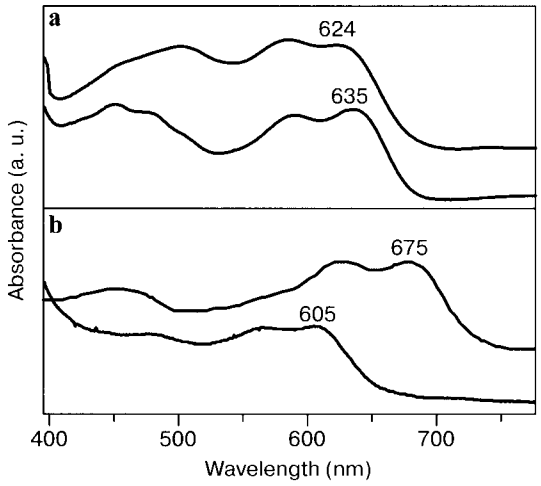

Fig. 2. Comparison of optical absorption spectra of paramagnetic photoactive flavoproteins recorded at room temperature. **a** *E. coli* CPD photolyase (upper curve) and *X. laevis* (6–4) photolyase (lower curve) (E. Schleicher et al., pers. commun.). **b** *C. reinhardtii* LOV1 C57M-675 (upper curve) (data taken from ref. 23) and *A. sativa* LOV2 C450A-605 (lower curve).

exhibit long-wavelength absorption maxima at 624 and 635 nm, respectively, which are assigned to the $D_0 \rightarrow D_1$ transitions. Weak shoulders that arise from the $D_0 \rightarrow D_2$ transitions are observed around 500 nm [38]. The shapes of the two photolyase spectra are quite different even though the flavin binding sites are essentially conserved in both enzymes. The pronounced spectral shifts in the optical absorption spectra therefore must be due to small structural dissimilarities which are not easily identified by X-ray crystallography with its typical spatial resolution that only in rare cases exceeds 0.15 nm. As a consequence, flavin radicals and their protonation state and/or type of bonding to the protein environment are not easily characterized solely on the basis of the optical absorption properties. This becomes obvious when one compares the optical absorption spectra of the photolyases to those from flavin radicals in photoactive LOV domains of algae and plants. Even larger spectral shifts of the $D_0 \rightarrow D_1$ transition are observed ranging from 675 nm in the case of LOV1 C57M-675 [23] to 605 nm in LOV2 C450A-605 [29] that preclude an easy assignment of the protonation state or the type of their bonding to the apoprotein, be it covalent or noncovalent. By EPR spectroscopy, both radicals have also been identified as neutral flavin radicals, i.e., a net-zero electronic charge characterizes their redox-active isoalloxazine rings. However, whereas the flavin radical in LOV2 C450A is clearly protonated at N(5) (again, this has been confirmed by pulsed ENDOR spectroscopy [unpubl. results]) and noncovalently bound to the LOV2 domain, the flavin species in LOV1 C57M-675 is covalently linked to its LOV1 domain by an alkyl bridge attached to N(5) (as confirmed by EPR [28], mass spectrometry and X-ray crystallography [23]). In the following, we turn to 360

GHz EPR spectroscopy to examine the g-tensors of the paramagnetic flavin species in both LOV domains with the goal to examine how g is influenced on the different types of flavin protonation and binding.

3.2 X-Band and 360 GHz EPR Spectroscopy

In Fig. 3, a comparison of the 9.66 GHz continuous-wave EPR spectra of LOV1 C57M-675 and LOV2 C450A-605 recorded at $T = 150$ K is shown. Both proteins exhibit EPR spectra that are typical for aromatic organic radicals where the spectral line width is dominated by hyperfine interactions. As can be deduced from the fairly symmetric overall line shapes of both signals, the Zeeman anisotropy as determined by the g-tensor is small at X-band. In neutral flavin radicals, the dominant hyperfine couplings are those arising from the nitrogens N(5) and N(10), the α-proton H(5) if present or any other β-proton at N(5), the β-protons at C(1′) and C(8α), and the α-proton H(6) [24, 39–41]. Most of them are strongly anisotropic, and given the relatively large size of the LOV domains [21, 32], the overall molecular motion of the protein is not rapid enough so that the hyperfine anisotropies persist even if the spectra are collected at room temperature. This results in strongly inhomogeneously broadened EPR signals with mostly unresolved hyperfine structure [28, 29]. Hence, on the basis of the spectral line shape of the X-band EPR signal alone, the different chemical nature of the two flavin radicals in the LOV1 and LOV2 domains cannot be deduced. Also

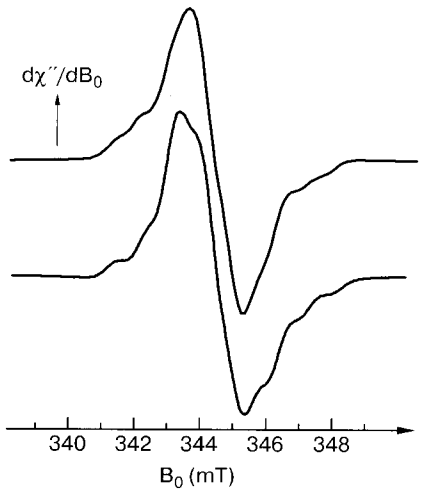

Fig. 3. Comparison of the continuous-wave EPR spectra of LOV1 C57M-675 (upper trace) and LOV2 C450A-605 (lower trace) recorded at 9.66 and 9.43 GHz, respectively, at a temperature of 150 K. The magnetic-field axis of the LOV2 C450A-605 spectrum has been multiplied by 9.66/9.43 in order to compensate the spectral shift due to the different microwave frequency used in comparison to LOV1 C57M-675.

the peak-to-peak spectral line widths are not sufficient to decide whether the radicals are protonated at N(5) or not, because the protons at C(1′), depending on the orientation of the flavin's ribityl side chain, may assume isotropic hyperfine couplings with values ranging from about zero up to 22 MHz. Deuteration of the buffer in order to replace the exchangeable protons H(5) and H(3) for deuterons may yield further information. An enrichment of D_2-FMN to a yield higher than 80% is, however, sometimes difficult to achieve if the flavin cofactor is not easily accessible to the solvent.

To yield a measure of the overall electronic structure of a flavin radical as reflected by its *g*-tensor, EPR experiments at higher microwave frequencies and correspondingly stronger magnetic fields are required. Under such conditions, the Zeeman anisotropy becomes the dominant interaction. The hyperfine couplings, which are typically strongly influenced by local protein–cofactor interactions, will then only contribute to the inhomogeneous line broadening of the EPR signal. In Fig. 4, the 360.03 GHz continuous-wave detected EPR spectrum of LOV1 C57M-675 recorded at $T = 160$ K is shown. The anisotropic spectrum exhibits the characteristic shape of a randomly oriented radical with well-resolved orthorhombic *g*-tensor components. Resolving very small *g*-anisotropies (as expected for flavin radicals [36]) is a major advantage of EPR measurements at resonance magnetic fields far beyond those of commercially available EPR spectrometers

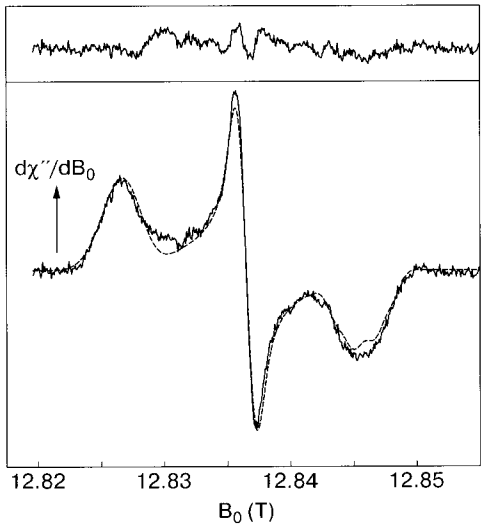

Fig. 4. Calculated (dashed line) and experimental (solid line) 360.03 GHz EPR spectrum of the flavin radical of LOV1 C57M-675 from *C. reinhardtii*. The difference between simulation and experiment is depicted by the trace at the top of the figure. The simulations have been obtained by least-squares fittings of spectral simulations to the experimental data using the *g* and hyperfine data compiled in Table 1. Experimental conditions: sample volume, 0.5 µl placed onto the curved mirror of a Fabry-Pérot resonator; microwave power, 0.3 mW; lock-in modulation frequency, 1.63 kHz; lock-in modulation amplitude, 0.4 mT.

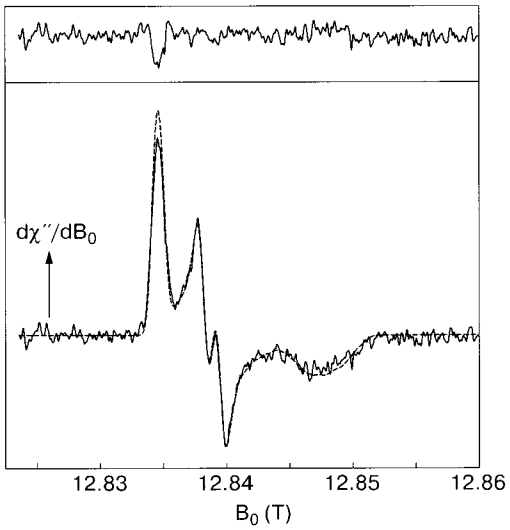

Fig. 5. Calculated (dashed line) and experimental (solid line) 360.04 GHz EPR spectrum of the flavin radical of LOV2 C450A-605 from *A. sativa*. The difference between simulation and experiment is depicted by the trace at the top of the figure. The simulations have been obtained by least-squares fittings of spectral simulations to the experimental data using the g and hyperfine data compiled in Table 1. Experimental conditions: sample volume, 9 µl placed in a sample holder; microwave power, 0.2 mW; lock-in modulation frequency, 6.17 kHz; lock-in modulation amplitude, 0.6 mT.

operating at X-, Q-, or W-band frequencies. Benefiting from the high spectral resolution, we were able to measure the principal values of the g-tensor of LOV1 C57M-675 with high accuracy. Least-squares fittings of spectral simulations to the experimental data yielded the following values: $g_X = 2.00554(5)$, $g_Y = 2.00391(5)$, and $g_Z = 2.00247(7)$, resulting in an average value of $g_{iso} = 2.00397(6)$. The error margins for g_X and g_Y, $\pm 5 \cdot 10^{-5}$, are a result of uncertainties in the isotropic g-value of the Mn(II)/MgO magnetic-field standard [35]. Due to this fact, the difference between the principal components of g obtained from the same spectrum can be assessed with higher precision ($\pm 2 \cdot 10^{-5}$). At the high-field edge of the spectrum, unresolved hyperfine interactions originating mostly from the nitrogens N(5) and N(10) broaden the EPR line and lead to further uncertainties in the determination of g_Z. For the simulations, the mostly isotropic proton hyperfine coupling of the two β-protons near N(5) as determined from pulsed X-band ENDOR spectroscopy have been taken into account [28]. All simulation parameters that enter the calculations have been compiled in Table 1.

In Fig. 5, the 360.04 GHz continuous-wave EPR spectrum of LOV2 C450A-605 recorded at $T = 160$ K is shown. Using the same procedure outlined above, the principal components of g have been extracted: $g_X = 2.00427(5)$, $g_Y = 2.00360(5)$, and $g_Z = 2.00220(7)$, yielding an average value of $g_{iso} = 2.00336(6)$. For the simulations, the proton hyperfine coupling of the α-proton H(5) as determined by pulsed X-band ENDOR spectroscopy (E. Schleicher et al., pers.

commun.) has been taken into account. As in the case of the photolyases [26, 27, 36], the 360 GHz EPR spectrum of the flavin radical in LOV2 C450A-605 shows a splitting at the resonance position of g_Y (see Fig. 5), which is attributed to the hyperfine coupling of the strongly coupled H(5), the assignment being based on quantum-chemical calculations [39] and pulsed ENDOR experiments that yielded the hyperfine principal components A_x(H(5)) = (−)0.49 mT, A_y(H(5)) = (−)1.32 mT, and A_z(H(5)) = (−)0.9 mT (x, y, and z are the principal axes of A(H(5))). The difference between the principal hyperfine component A_y(H(5)) and the splitting at g_Y is due to the rotation of the g-tensor about the angle $|\delta|$, which determines the orientation of the X- and Y-axes of g with respect to the x- and y-axes of A(H(5)). Assuming that Z and z are collinear and perpendicular to the molecular plane of the flavin's isoalloxazine ring, then from least-squares fittings of the 360-GHz EPR spectrum we obtain $|\delta| = (8\pm2)°$ for LOV2 C450A-605.

3.3. Comparison of the g-Tensors of LOV1 C57M-675 and LOV2 C450A-605

In Fig. 6, a comparison of the 360 GHz continuous-wave EPR spectra of LOV1 C57M-675 and LOV2 C450A-605 drawn on a g-scale is shown. It becomes immediately apparent that the overall spectral shape of LOV1 C57M-675 strongly deviates from those of previously published spectra obtained from the neutral flavin radicals in CPD photolyase [36] and (6–4) photolyase [27] and also from

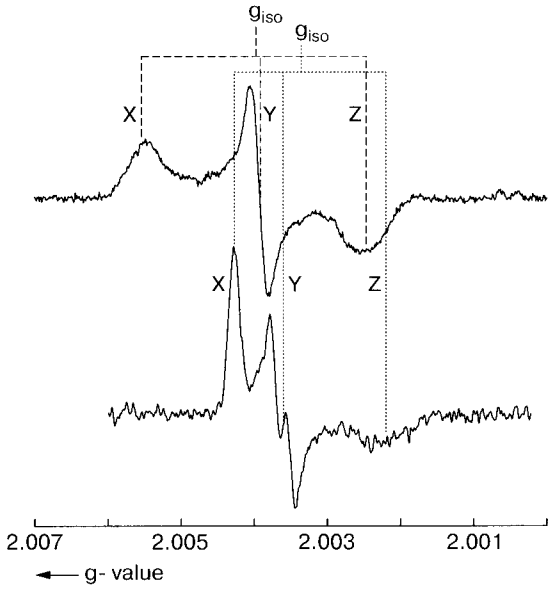

Fig. 6. Comparison of the FMN radicals in LOV1 C57M-675 (upper trace) and LOV2 C450A-605 (lower trace).

Table 2. Comparison of the g-tensor parameters of different flavin radicals obtained from 95 and 360 GHz EPR.

Parameter		Value for FADH$^{\bullet}$ in:		Value for:	
		E. coli CPD photolyase [25, 36]	*X. laevis* (6–4) photolyase [26, 27]	FMNH$^{\bullet}$ in *A. sativa* LOV2 C450A-605	FMN$^{\bullet}$ in *C. reinhardtii* LOV1 C57M-675
g-Tensor	g_X	2.00431(5)	2.00432(5)	2.00427(5)	2.00554(5)
	g_Y	2.00360(5)	2.00368(5)	2.00360(5)	2.00391(5)
	g_Z	2.00217(7)	2.00218(7)	2.00220(7)	2.00247(7)
g_{iso}		2.00336(6)	2.00339(6)	2.00336(6)	2.00397(6)
$g_X - g_Y$		$7.1(2) \cdot 10^{-4}$	$6.4(2) \cdot 10^{-4}$	$6.7(2) \cdot 10^{-4}$	$16(2) \cdot 10^{-4}$
$\|\delta\|$		(17±2)°	(29±2)°	(8±2)°	n.a.

that of LOV2 C450A-605 (Fig. 5). The g-tensor assumes a more symmetric rhombic pattern, with $g_Y \approx (g_X + g_Z)/2$, i.e., $g_Y \approx g_{iso}$ (see Table 2). Furthermore, no splitting of the resonances at g_Y is observed unlike the photolyases and also LOV2 C450A-605. Rather, all transitions are significantly broadened, which is due to the strong and not very anisotropic hyperfine couplings of the two β-protons at C(5′), for which an average coupling of (−)0.62 mT has been reported [28].

A comparison of the g-tensor from LOV1 C57M-675 with those of the photolyases [27, 36] and of LOV2 C450A-605 reveals that all principal components g_i ($i = X, Y, Z$) of LOV1 C57M-675 are shifted towards larger values with respect to their counterparts in the other proteins (Table 2). This is most likely due to the presence of the sulfur atom from the methionine residue that as has been shown by a X-ray crystal structural analysis [23] assumes a position above the π-plane of the flavin chromophore. The larger g_i values therefore are a result of an increased spin–orbit coupling due to the heavy sulfur atom interacting with the unpaired electron spin.

The spectral shape of the LOV2 C450A-605 EPR signal, the position of the resonances and the splitting at the central spectral region near g_Y are very similar to the spectra reported for the neutral flavin radicals of CPD photolyase and (6–4) photolyase (Table 2). Within the error margins, the g-components are identical compared to those in the photolyases with the exception of the g_Y value, which assumes a slightly larger value than in (6–4) photolyase. The same g_Y principal value, 2.00360(5), has been observed in CPD photolyase. We have shown previously that alterations of the flavin cofactor surroundings appear to affect the g_Y principal value more than g_X. Also the orientation of the principal axes of g has been shown to react sensitively on minor changes in the protein surroundings, ranging from about |8°| in LOV2 C450A-605 to |29°| in (6–4) photolyase [26]. The latter effect, however, is far from being understood on the molecular level. On the other hand, g_X is known to react more sensitively towards changes in the polarity and/or hydrogen-bonding situation in nitroxide spin

labels [42], quinones [43–45] and tyrosines [46]. This difference presumably lies in the different symmetry of flavins with respect to nitroxides or para-quinones. The latter have a well-defined symmetry axis with X aligned along the N−O or C=O bonds, respectively, and there are high unpaired electron-spin densities on the oxygens. Hence, they are particularly sensitive to changes of hydrogen bonding in this direction. Flavins, on the other hand, have much lower symmetry with the two carbonyl groups being meta-positioned. Furthermore, the unpaired electron-spin density in flavins is mostly localized on C(4a) and N(5) rather than on the two carbonyl groups [39]. This is a consequence of the more extended π-system in flavins as compared with nitroxides or tyrosines. Hence, hydrogen bonding to H(5) is also expected to alter the spin distribution on the isoalloxazine ring. Taken together, it may well be that in neutral flavin radicals the g_Y principal value probes more sensitively the changes in the cofactor–protein binding situation and the polarity profile in the cofactor surroundings than g_X. Accordingly, similar g principal components in LOV2 C450A-605 and CPD photolyase imply that the protein surroundings that noncovalently bind the flavin are also closely similar in both proteins. This conclusion, however, seems not to be justified given the articulate differences in the optical absorption spectra of CPD photolyase and LOV2 C450A-605 (Fig. 2). Hence, it appears that the g-tensor of a flavin neutral radical reflects a coarse overall binding situation to the protein, its value being the sum of many individually smaller factors (hydrogen bonds, π-stacking, Coulombic interactions) that add up. This makes the identification of individual contributions more difficult, but in turn displays the robustness of the g-tensor as a measure of the overall electronic situation, i.e., neutral covalently bound flavin radical versus neutral N(5)-alkylated flavin radical. Thus, a characterization of the g-tensor of a flavin is particularly beneficial in cases where vastly different optical absorption properties preclude a direct assignment.

4 Conclusions

We have demonstrated that the g-tensor of a flavin reflects the overall electronic structure on the redox-active isoalloxazine ring and thus is potentially an appropriate property by which chemically different flavin radicals may be distinguished. Clearly, future studies using high-microwave-frequency and high-magnetic-field EPR need to be carried out to characterize other types of flavin radicals, such as C(8α)-linked or C(6)-linked chromophores in order to fully understand the diversification of the g-tensor when comparing different flavoproteins.

Acknowledgments

It is a pleasure to dedicate this contribution to Klaus Möbius on the occasion of his 70th birthday. Klaus is not only an outstanding scientist, he is also a creative teacher and a stimulating conversationalist. Those of us who had the chance

to work closely together with him are thankful that he shared his deep understanding of physical laws and principles with us. Klaus very often surprised us with a reformulation of spectroscopic concepts which frequently led to the introduction of new EPR techniques and methods boosting the development in this field. Based on a broadly educated humanity, Klaus' interest in the world is not limited to its physical description but also encompasses his social environment and its problems. Following Brecht's words "Denken ist etwas, was auf Schwierigkeiten folgt und dem Handeln vorausgeht" (Translation: "Thinking is something which follows problems and precedes action"), Klaus approaches problems not only as a scientist but also by his personal dedication. His engagement for Russian scientists after the collapse of the Soviet Union is only one example among numerous others for his committed way of living. We are grateful to Klaus for making the 360 GHz EPR spectrometer at the FU Berlin available for us to obtain the results presented in this contribution.

This study was supported by grants from the Deutsche Forschungsgemeinschaft (SFB 498, projects A2 (S.W.) and B7 (R.B., S.W.), SFB 533, project A5 (A.B., M.F., G.R.), and FOR-526, projects TP2 and TP6). We also thank Ulrike Stier (Bad Soden) and the Hans Fischer Gesellschaft e.V. for generously sponsoring this research work.

References

1. Karrer P., Köbner T., Salomon H., Zehender F.: Helv. Chim. Acta **18**, 266–272 (1935)
2. Karrer P., Schöpp K., Benz F.: Helv. Chim. Acta **18**, 426–429 (1935)
3. Massey V.: Biochem. Soc. Trans. **28**, 283–296 (2000)
4. Miller S.M., Massey V., Ballou D., Williams C.H., Distefano M.D., Moore M.J., Walsh C.T.: Biochemistry **29**, 2831–2841 (1990)
5. Briggs W.R., Huala E.: Annu. Rev. Cell Dev. Biol. **15**, 33–62 (1999)
6. Christie J.M., Briggs W.R.: J. Biol. Chem. **276**, 11457–11460 (2001)
7. Devlin P.F., Kay S.A.: Annu. Rev. Physiol. **63**, 677–694 (2001)
8. Lin C., Shalitin D.: Annu. Rev. Plant Biol. **54**, 469–496 (2003)
9. Sancar A.: Chem. Rev. **103**, 2203–2237 (2003)
10. Lin C., Todo T.: Genome Biol. **6**, 220 (2005)
11. Weber S.: Biochim. Biophys. Acta **1707**, 1–23 (2005)
12. Essen L.-O., Klar T.: Cell Mol. Life Sci. **63**, 1266–1277 (2006)
13. Mewies M., McIntire W.S., Scrutton N.S.: Protein Sci. **7**, 7–20 (1998)
14. Edmondson D.E., Newton-Vinson P.: Antioxid. Redox Signal. **3**, 789–806 (2001)
15. Wagner M.A., Khanna P., Jorns M.S.: Biochemistry **38**, 5588–5595 (1999)
16. Fraaije M.W., van den Heuvel R.H.H., van Berkel W.J.H., Mattevi A.: J. Biol. Chem. **274**, 35514–35520 (1999)
17. Hassan-Abdallah A., Zhao G., Jorns M.S.: Biochemistry **45**, 9454–9462 (2006)
18. Lim L.W., Shamala N., Mathews F.S., Steenkamp D.J., Hamlin R., Xuong N.H.: J. Biol. Chem. **261**, 15140–15146 (1986)
19. Huang L., Scrutton N.S., Hille R.: J. Biol. Chem. **271**, 13401–13406 (1996)
20. Salomon M., Eisenreich W., Dürr H., Schleicher E., Knieb E., Massey V., Rüdiger W., Müller F., Bacher A., Richter G.: Proc. Natl. Acad. Sci. USA **98**, 12357–12361 (2001)
21. Crosson S., Moffat K.: Proc. Natl. Acad. Sci. USA **98**, 2995–3000 (2001)
22. Choong Y.S., Massey V.: J. Biol. Chem. **256**, 8671–8678 (1981)
23. Kottke T., Dick B., Fedorov R., Schlichting I., Deutzmann R., Hegemann P.: Biochemistry **42**, 9854–9862 (2003)

24. Kay C.W.M., Feicht R., Schulz K., Sadewater P., Sancar A., Bacher A., Möbius K., Richter G., Weber S.: Biochemistry **38**, 16740–16748 (1999)
25. Kay C.W.M., Bittl R., Bacher A., Richter G., Weber S.: J. Am. Chem. Soc. **127**, 10780–10781 (2005)
26. Kay C.W.M., Schleicher E., Hitomi K., Todo T., Bittl R., Weber S.: Magn. Reson. Chem. **43**, S96–S102 (2005)
27. Schnegg A., Kay C.W.M., Schleicher E., Hitomi K., Todo T., Möbius K., Weber S.: Mol. Phys. **104**, 1627–1633 (2006)
28. Bittl R., Kay C.W.M., Weber S., Hegemann P.: Biochemistry **42**, 8506–8512 (2003)
29. Kay C.W.M., Schleicher E., Kuppig A., Hofner H., Rüdiger W., Schleicher M., Fischer M., Bacher A., Weber S., Richter G.: J. Biol. Chem. **278**, 10973–10982 (2003)
30. Richter G., Weber S., Römisch W., Bacher A., Fischer M., Eisenreich W.: J. Am. Chem. Soc. **127**, 17245–17252 (2005)
31. Crosson S., Moffat K.: Plant Cell **14**, 1067–1075 (2002)
32. Fedorov R., Schlichting I., Hartmann E., Domratcheva T., Fuhrmann M., Hegemann P.: Biophys. J. **84**, 2474–2482 (2003)
33. Holzer W., Penzkofer A., Fuhrmann M., Hegemann P.: Photochem. Photobiol. **75**, 479–487 (2002)
34. Fuchs M.R., Prisner T.F., Möbius K.: Rev. Sci. Instrum. **70**, 3681–3683 (1999)
35. Burghaus O., Rohrer M., Götzinger T., Plato M., Möbius K.: Meas. Sci. Technol. **3**, 765–774 (1992)
36. Fuchs M., Schleicher E., Schnegg A., Kay C.W.M., Törring J.T., Bittl R., Bacher A., Richter G., Möbius K., Weber S.: J. Phys. Chem. B **106**, 8885–8890 (2002)
37. Weber S., Kay C.W.M., Bacher A., Richter G., Bittl R.: ChemPhysChem **6**, 292–299 (2005)
38. Schelvis J.P.M., Ramsey M., Sokolova O., Tavares C., Cecala C., Connell K., Wagner S., Gindt Y.M.: J. Phys. Chem. B **107**, 12352–12362 (2003)
39. Weber S., Möbius K., Richter G., Kay C.W.M.: J. Am. Chem. Soc. **123**, 3790–3798 (2001)
40. García J.I., Medina M., Sancho J., Alonso P.J., Gómez-Moreno C., Mayoral J.A., Martínez J.I.: J. Phys. Chem. A **106**, 4729–4735 (2002)
41. Barquera B., Morgan J.E., Lukoyanov D., Scholes C.P., Gennis R.B., Nilges M.J.: J. Am. Chem. Soc. **125**, 265–275 (2003)
42. Kawamura T., Matsunami S., Yonezawa T.: Bull. Chem. Soc. Jpn. **40**, 1111–1115 (1967)
43. Burghaus O., Plato M., Rohrer M., Möbius K., MacMillan F., Lubitz W.: J. Phys. Chem. **97**, 7639–7647 (1993)
44. Isaacson R.A., Lendzian F., Abresch E.C., Lubitz W., Feher G.: Biophys. J. **69**, 311–322 (1995)
45. Sinnecker S., Reijerse E., Neese F., Lubitz W.: J. Am. Chem. Soc. **126**, 3280–3290 (2004)
46. Un S., Atta M., Fontecave M., Rutherford A.W.: J. Am. Chem. Soc. **117**, 10713–10719 (1995)

Authors' address: Stefan Weber, Fachbereich Physik, Freie Universität Berlin, Arnimallee 14, 14195 Berlin, Germany
E-mail: Stefan.Weber@physik.fu-berlin.de